J. Indian Inst. Sci. 63 (A), Sept. 1981, Pp. 213–226

Effect of graphite size and spacing on the elastic constants of spheroidal graphite cast iron : an analytical approach

S. SEETHARAMU*, MALUR N. SRINIVASAN* AND P. D. MANGALGIRI**
Indian Institute of Science, Bangalore 560 012, India.

Abstract

The effect of graphite size and spacing upon the elastic constants of spheroidal graphite cast iron has been studied for different graphite-matrix interface conditions through a finite element analysis of two dimensional idealized configuration of inclusion and matrix. The interface conditions considered cover situations ranging from complete rigidity to complete elastic deformation of the inclusion. It has been attempted to throw light on the probable modes of elastic deformation of graphite in spheroidal graphite iron castings based on comparison of analytical values with experimentally determined values available in the literature. While the interfacial conditions considered appear to influence the overall elastic modulus when the inclusion is hard, such effect is shown to be relatively insignificant for soft inclusions such as graphite.

Key words: Cast iron, elastic constants, finite element method, graphite–matrix interface.

1. Introduction

Graphite configuration in cast iron plays an important role in deciding the mechanical behaviour of the alloy. While the strength and toughness of cast iron are relatively low when graphite occurs in flake form, the formation of graphite in spheroidal shape leads to considerable improvement in these properties, the values sometimes approaching those of steel[1]. However, the elastic modulus of spheroidal graphite cast iron is significantly lower than that of steel[1]. As graphite is essentially a second phase particle in a steel-like matrix in cast iron, this phase may be considered to be predominantly responsible for lowering the elastic modulus. As the graphite configuration in the microstructure is determined by the shape, size and spacing of graphite particles, it would be of value to understand the influence of these factors upon the elastic constants of the alloy. While the effect of graphite shape has been studied earlier[2,3], the influence of size and spacing of spheroidal graphite has not been systematically examined. In view of this, a finite element analysis was carried out to study the load transfer around an inclusion

*Department of Mechanical Engineering
**Department of Aeronautical Engineering

under different conditions at the inclusion-matrix interface and the results obtained were employed to estimate the effect of size and spacing of graphite upon the elastic constants of spheroidal graphite cast iron. This approach appears to be useful in throwing light on the probable modes of load transfer through graphite in practical situations. In what follows, a two-dimensional idealization utilized is presented and the results are compared with experimental values.

2. Formulation

The material is considered to be consisting of two phases, *i.e.*, the matrix and the inclusion. Both the phases are considered to be isotropic and homogeneous. Further, the inclusion is considered to be uniformly distributed throughout the matrix so that the whole material may be assumed to consist of microscopic unit cells each containing an

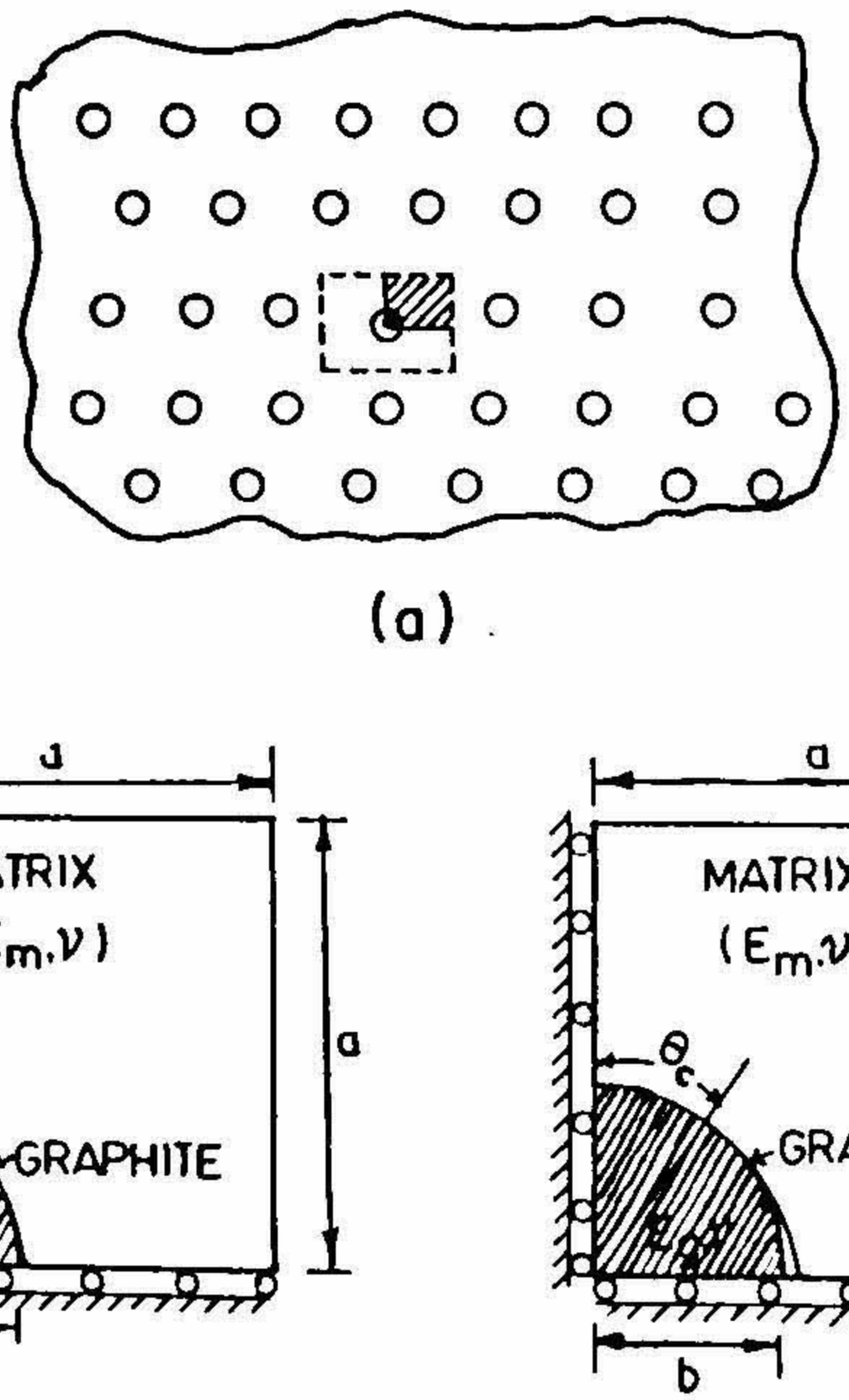

FIG. 1. Schematic representation of the unit cell.

inclusion at the centre. A two-dimensional model is used so that the matrix is taken as a large sheet in which circular inclusions are embedded (Fig. 1*a*). Since all cells are identical, only one such cell needs to be analysed (Figs. 1*b* and 1*c*). The analysis is carried out for various sizes of the inclusion. The various boundary conditions at the inclusion-matrix interface studied in the present work are as follows :

Case 1

The inclusion-matrix interface is assumed to be bonded. The elastic properties of graphite are assigned to the inclusion and that of steel to the matrix (Fig. 1*a*).

Case 2

The interface is assumed to be load-free, *i.e.*, displacement occurs along the interface and the load transfer across the inclusion is zero as in the case of a void.

Case 3

The interface is assumed to be rigid, *i.e.*, no displacement of the interface occurs during loading. This corresponds to an inclusion of very high elastic modulus bonded to the matrix.

During loading, it is also likely that the inclusion may be partially bonded to the matrix. The following interface conditions are also investigated to cover such a possibility (Fig. 1*c*).

Case 4

The inclusion, to which the properties of graphite are assigned, is assumed to be in partial contact with the interface, *i.e.*, a part of the interface will deform with the matrix and part of the interface is load-free. In the load-free part of the interface, the matrix and inclusion are allowed to deform separately under the applied load.

Case 5

The inclusion is again assumed to be in partial contact with the interface but the inclusion is assumed to be rigid. This corresponds to an inclusion with high modulus of elasticity but unbonded to the matrix over part of the interface under load.

The sizes of the inclusion and the matrix cavity in which the former is embedded are assumed to be the same in Cases 4 and 5 so that the angle of contact does not change with the load[4-6]. A parametric study is made by changing the geometric and material parameters as follows :

(i) The b/a ratio is varied from 0·1 to 0·5 in each case, where $2b$ is the mean diameter of the inclusion and $2a$ is the mean interparticle spacing (Figs. 1*b* and 1*c*). This would correspond to variation in the area fraction (volume fraction) of inclusion from about 1% to about 20%.

(ii) In Case 1, the elastic modulus of the inclusion (graphite)[8-9] E_p is varied from 3·5 to 31 GNm^{-2}. The elastic modulus of the matrix[1] E_m is assumed to be 207 GNm^{-2}. Thus E_p/E_m is varied from about 0·017 to 0·15. The Poisson's ratio is assumed to be 0·3 both for the matrix and the inclusion. It is to be further noted that for a void (Case 2), $E_p/E_m = 0$ and for rigid inclusion (Case 3), $E_p/E_m \to \infty$.

(iii) The angle of contact θ_p (Fig. 1*c*) is varied from 15° to 60° in Case 4 and 10° to 50° in Case 5. The angle of contact is reported to be in the range of 10° to 20° in Case 4 and about 53° in Case 5 for an unbonded inclusion in an infinite plate[4] and that the angle is likely to be marginally lower for a finite plate[6]. In the present work the angle of contact is varied over a fairly large range to cover such situations as well as partially bonded cases.

3. Procedure

The unit cell is considered to be under biaxial loading by specifying displacements U_y and U_x on the edges BC and CD (Fig. 2). A finite element analysis based on displace-

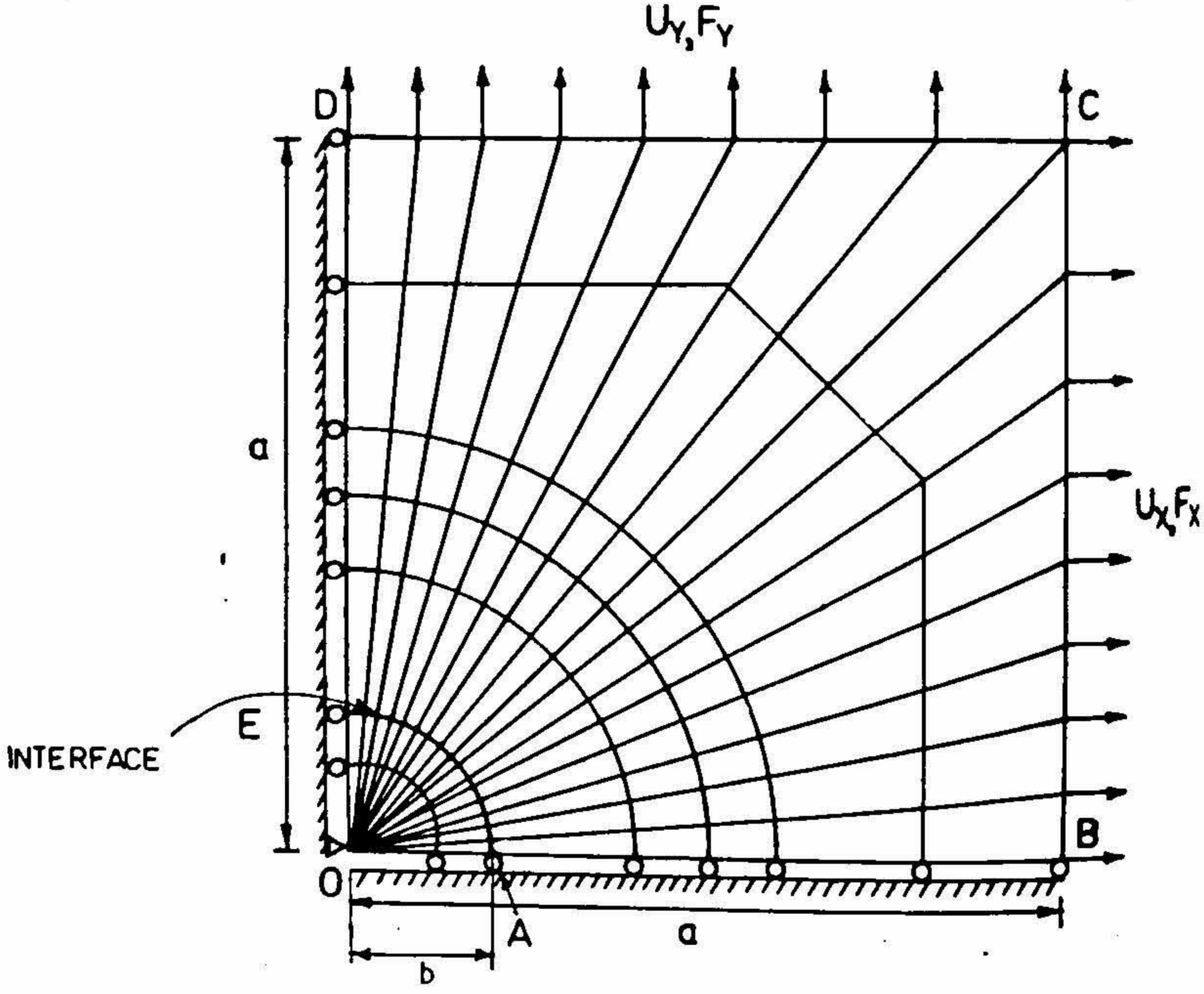

FIG. 2. Typical finite element meshes employed in the present work.
FIG. 2 (*a*). Elastic inclusion—Full contact.

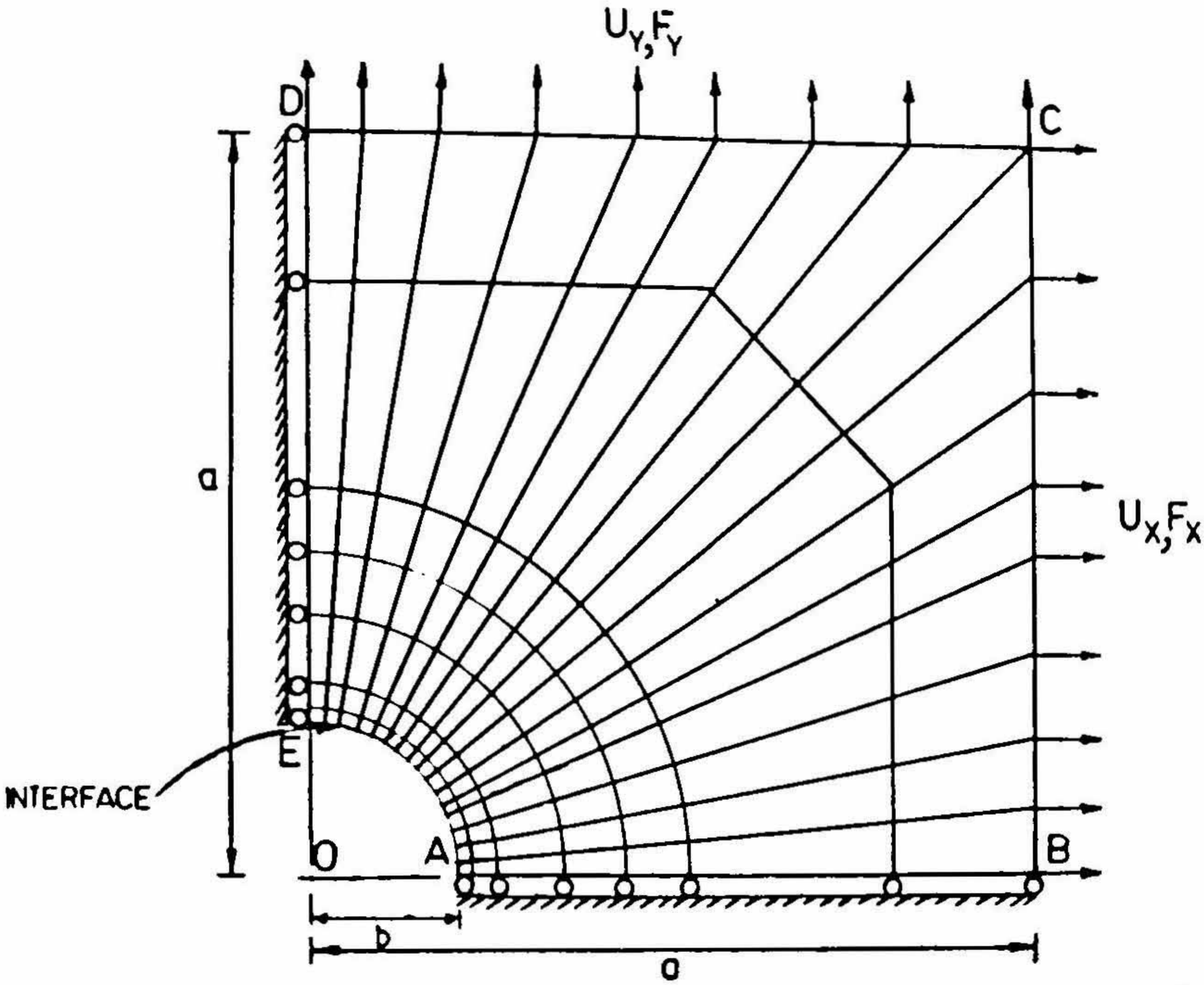

FIG. 2 (*b*). Rigid inclusion—Void.

ment formulation and using simple triangular and quadrilateral elements[7] as shown in fig. 2 is carried out to obtain the forces on the edges of the unit cell. The overall elastic constants E^* and ν^* of the matrix-inclusion combination were estimated by a procedure given in Appendix I.

4. Results

The E^*/E_m and ν^* values obtained by the finite element method in Cases 1–3 are plotted against b/a values in figs. 3 and 4. In fig. 5 is plotted the variation of E^*/E_m values with the angle of contact θ_c (Cases 4 and 5).

It can be observed from fig. 3 that while soft inclusions (Cases 1 and 2) tend to reduce the values of overall elastic modulus E^* compared to matrix elastic modulus E_m, hard inclusions (Case 3) tend to increase the value of E^*. These trends are more significantly noted when the b/a values are large, *i.e.*, at higher inclusion content.

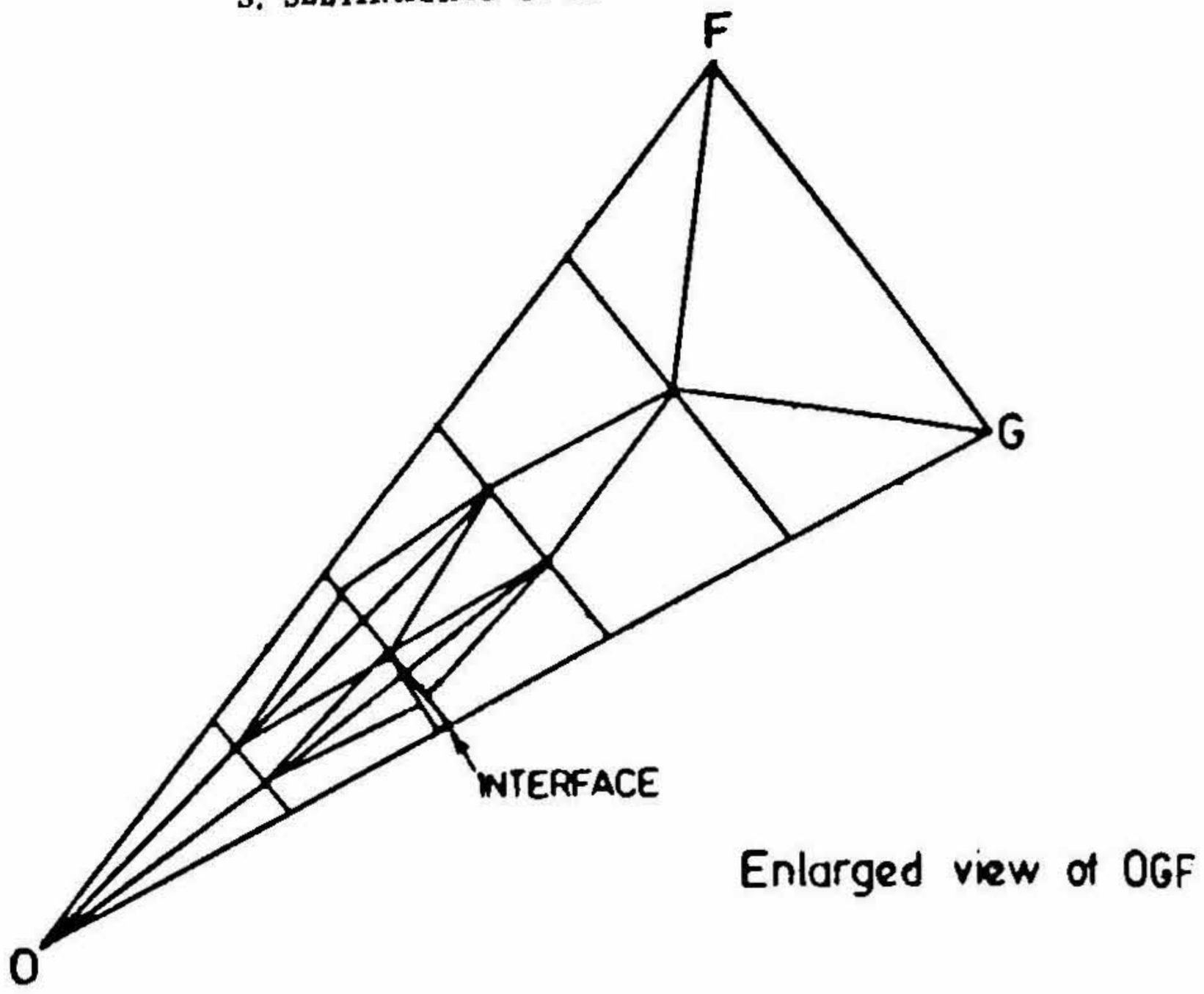

FIG. 2 (*c*). Elastic inclusion—Partial contact.

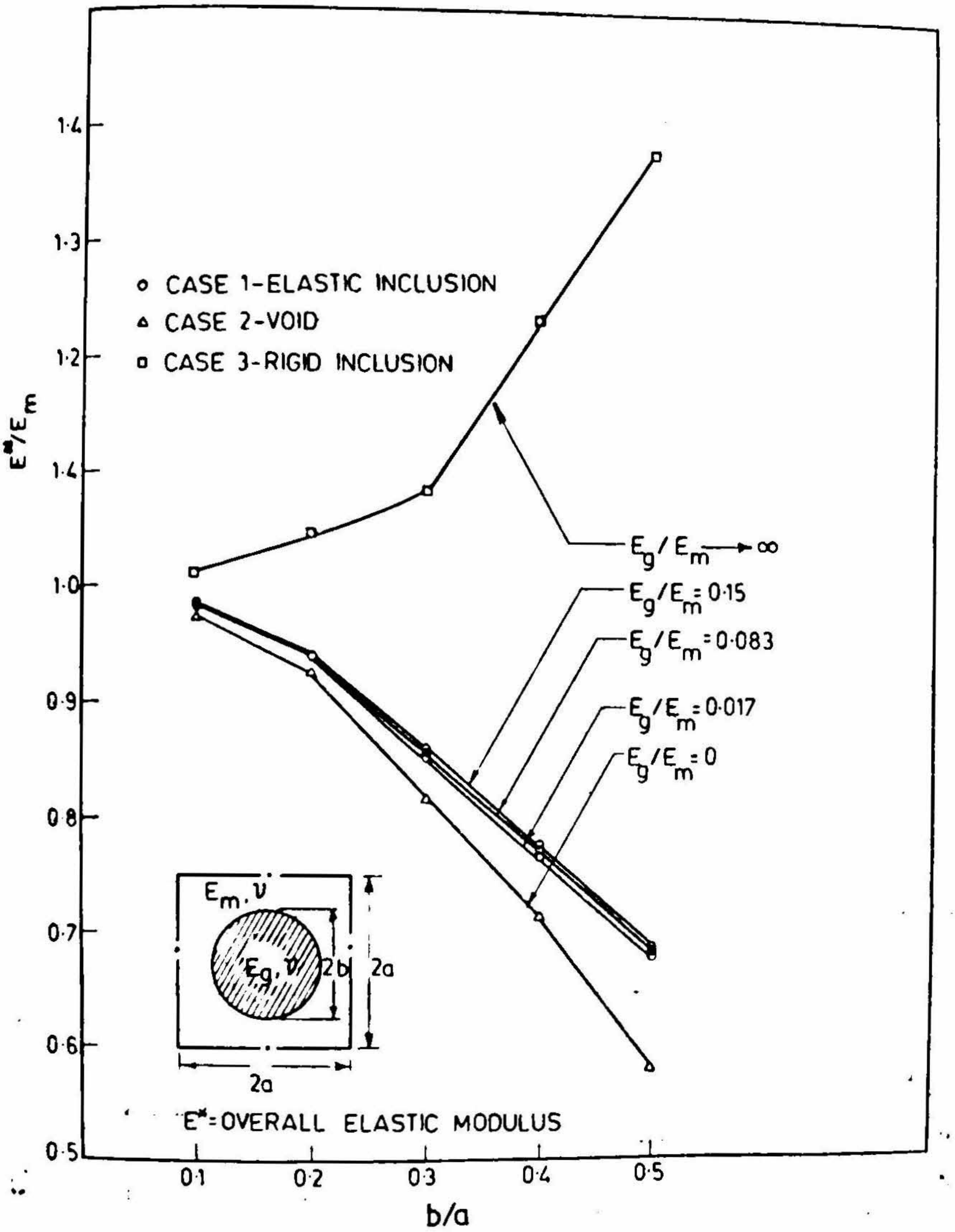

FIG. 3. Effect of *b/a* ratio upon overall elastic modulus.

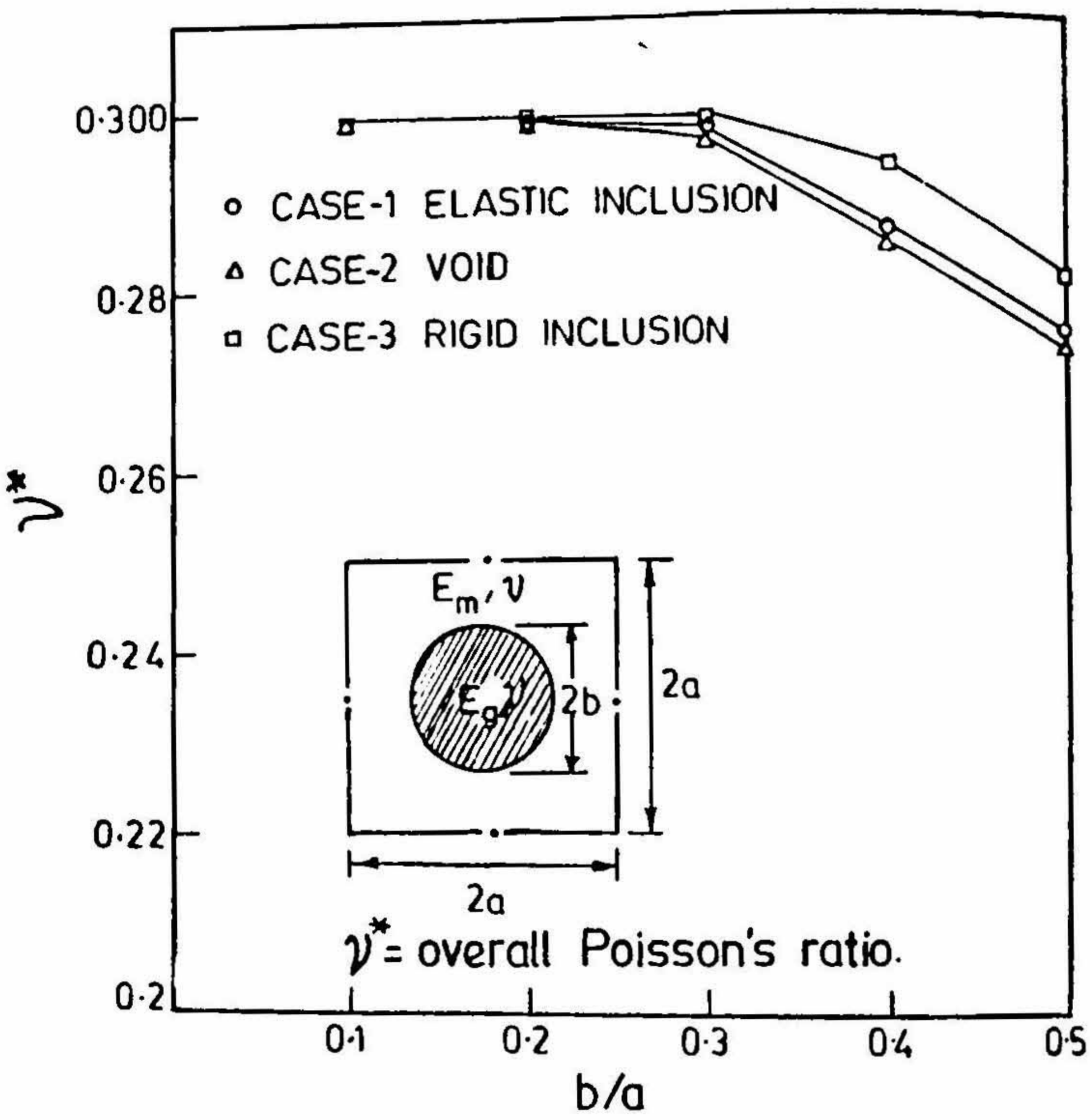

FIG. 4. Effect of *b/a* ratio upon overall Poisson's ratio.

When the inclusion is assumed to be in partial contact with the matrix, the E^* values appear to depend upon the elastic stiffness of the inclusion. It can be seen from fig. 5 that the angle of contact significantly influences the E^* values when the inclusion is hard ($E_g/E_m \to \infty$), while E^* values are only marginally affected for a soft inclusion ($E_g/E_m = 0{\cdot}083$). Further, the above trend appears to be more pronounced when the *b/a* values are large (Fig. 5).

4.1. *Utilization of analytical results for predicting the elastic constants in spheroidal graphite cast iron*

So far, the effects of inclusion size and spacing upon the elastic constants have been discussed in general terms. It will now be attempted to utilize these results to obtain

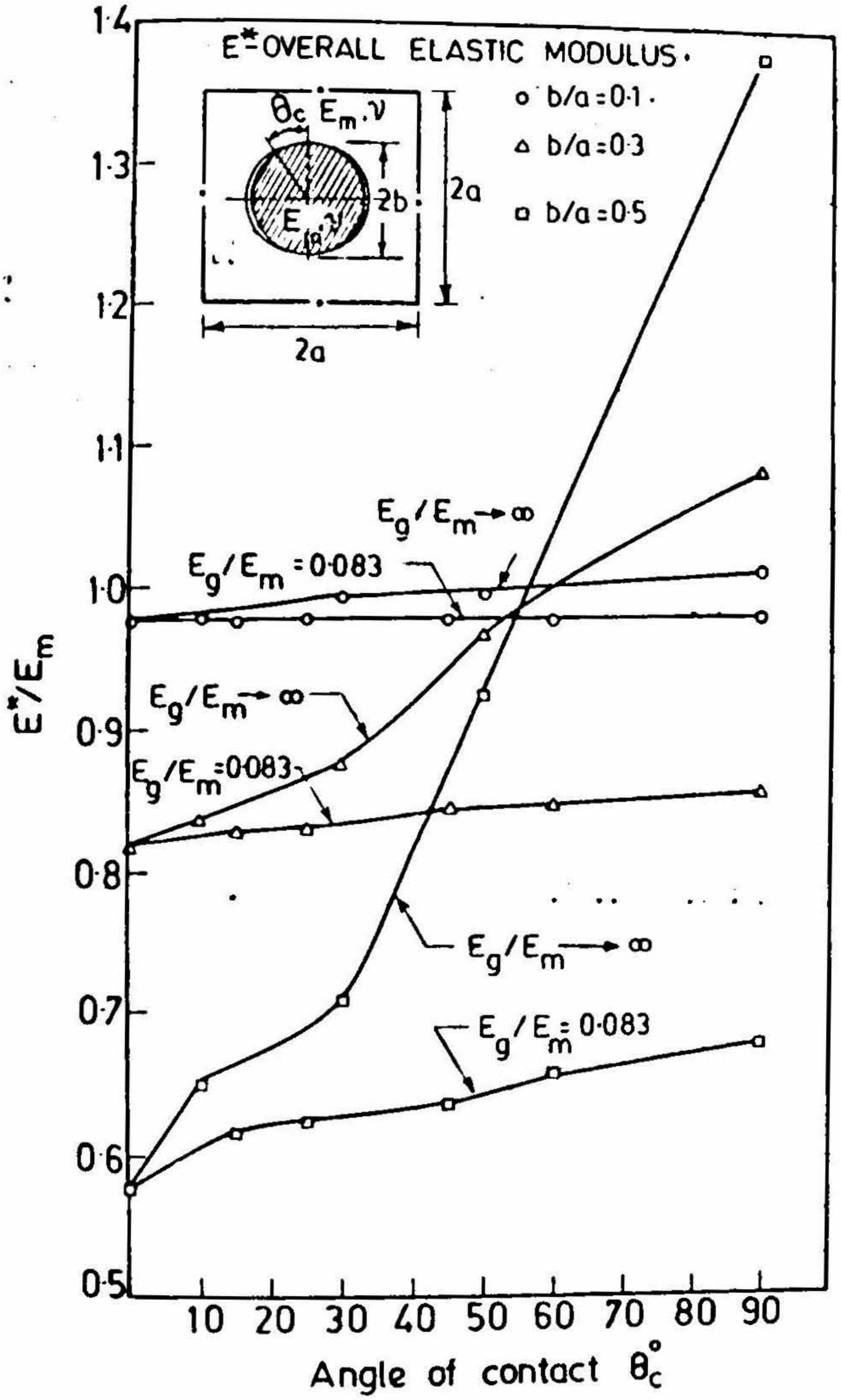

FIG. 5. Effect of angle of contact upon overall elastic modulus.

the estimates of elastic constants, and compare them with the reported variations in experimentally determined E values of spheroidal graphite cast iron. Before attempting this, however, a knowledge of graphite-matrix interface conditions as well as values of b/a ratio applicable to the experimental castings would be essential. It is well known that the graphite particles possess very low strength and stiffness (strength ≈ 20 MNm^{-2} and $E_g \approx 5$–20 GNm^{-2})[8,9] and are initially bonded to the matrix. This would correspond to E_g/E_m values in the range 0·025 to 0·1. Further, for graphite content in spheroidal graphite cast iron in the range of 3·0% to about 4·0% (weight per cent) the volume fraction of graphite V_g can be calculated to be in the range of 9 to 12%, based on the density values of steel (7·8 g/cc) and graphite (2·25 g/cc)[1]. As the present analysis is restricted to two dimensions, the volume fraction of graphite (V_g) is assumed to be equal to the area fraction. In the two-dimensional unit cell considered in the present work (Fig. 1), $V_g = \pi b^2/4a^2$ where $2b$ is the mean diameter of graphite and $2a$ is the mean interparticle spacing. So, $b/a = 1{\cdot}128\sqrt{V_g}$. Corresponding to the range of variation in volume fraction of graphite (*i.e.*, 9% to 12%) the b/a ratio calculated is in the range of 0·34 to 0·39.

The above calculations assume uniform distribution of graphite nodules of the same size. However, in practice, the size and spacing of graphite nodules vary considerably in a given casting. Also, in addition to the carbon content, factors like inoculation practice and cooling rate of the casting also affect the size and spacing of the graphite nodule. Hence for practical situations only an average value of b/a ratio can be consi-

Table I

Variation of b/a ratio with nodule count in spheroidal graphite iron castings[10]

No.	Graphite nodule count per mm^2	Average nodule diameter mm	b/a
1	50	0·043	0·304
2	96	0·032	0·314
3	102	0·031	0·313
4	108	0·029	0·301
5	118	0·030	0·326
6	127	0·027	0·304
7	167	0·029	0·375
8	186	0·029	0·396
9	212	0·026	0·379
10	240	0·028	0·434
11	256	0·023	0·368
12	275	0·023	0·381

dered. In table I is shown the variation of average b/a ratio measured in castings having different graphite nodule counts[10]. It can be easily seen that the b/a ratio increases with increase in graphite nodule count.

In view of the factors discussed above, b/a ratio in the range of 0·3 to 0·4 appears to be suitable for practical spheroidal graphite iron castings. Corresponding to these b/a values, the values of overall elastic constants E^* and v^* can be derived from figs. 3 and 4. It can be seen that E^* decreases with increase in b/a ratio values and varies between 160 and 178 GNm^{-2} in Case 1, where the properties of graphite are assigned to the inclusion and the inclusion is assumed to be bonded to the matrix. The E^* values are not appreciably altered when the elastic modulus of graphite is varied over a narrow range (Case 1, Fig. 3). It can be further seen that for Case 2 (Fig. 3), where the interface is considered to be load-free as in the case of a void, the E^* values vary in the range of 149 to 170 GNm^{-2}. When the contact at the interface is assumed to be partial, it is found that the E^* values vary from about 159 to 176 GNm^{-2} when the angle of contact is 60° and the values are only marginally lowered when the angle of contact is decreased. The value of Poisson's ratio v^* varies in the range of 0·28 to 0·29 and is not appreciably affected by the interface boundary conditions. The values of elastic constants determined for different possibilities of graphite-matrix interface conditions considered (Cases 1, 2 and 4) agree fairly well with the experimentally reported results where values in the range of 151 to 170 GNm^{-2} and 0·26 to 0·28 have been reported for E^* and v^* respectively[11].

Further, the modulus of elasticity E^* is reported[12] to decrease with increase in graphite content and graphite nodule count. As increase in either the graphite content or the graphite nodule count would lead to higher b/a values, the trend in the results obtained in the present work agrees well with the trend in the reported experimentally determined results. In fig. 6, the E^* values are plotted against graphite content (weight) %, the latter bing estimated based on b/a values. It can be seen that the values obtained in the present work agree quite well with the previously published results[2].

It is to be further noted that the values of E^* and v^* can be reasonably well predicted in Case 2 where the interface is assumed to be load-free, *i.e.*, the inclusion is considered to be a void. This is because of the enormous differences in the elastic stiffness of the graphite and the matrix. Owing to the same reason there does not appear to be any significant load transfer across the graphite-matrix interface. The lack of significant differences in the value of elastic constant E^* under different interface conditions (for a given b/a value) suggests that a simple interfacial condition can be considered in further studies like three-dimensional analysis wherein consideration of complex boundary conditions such as those involved in partial contact is rather difficult.

The results obtained in the present work for rigid interface conditions (Case 3, Fig. 3) point out to the fact that higher E^* values are obtained when the inclusion has high

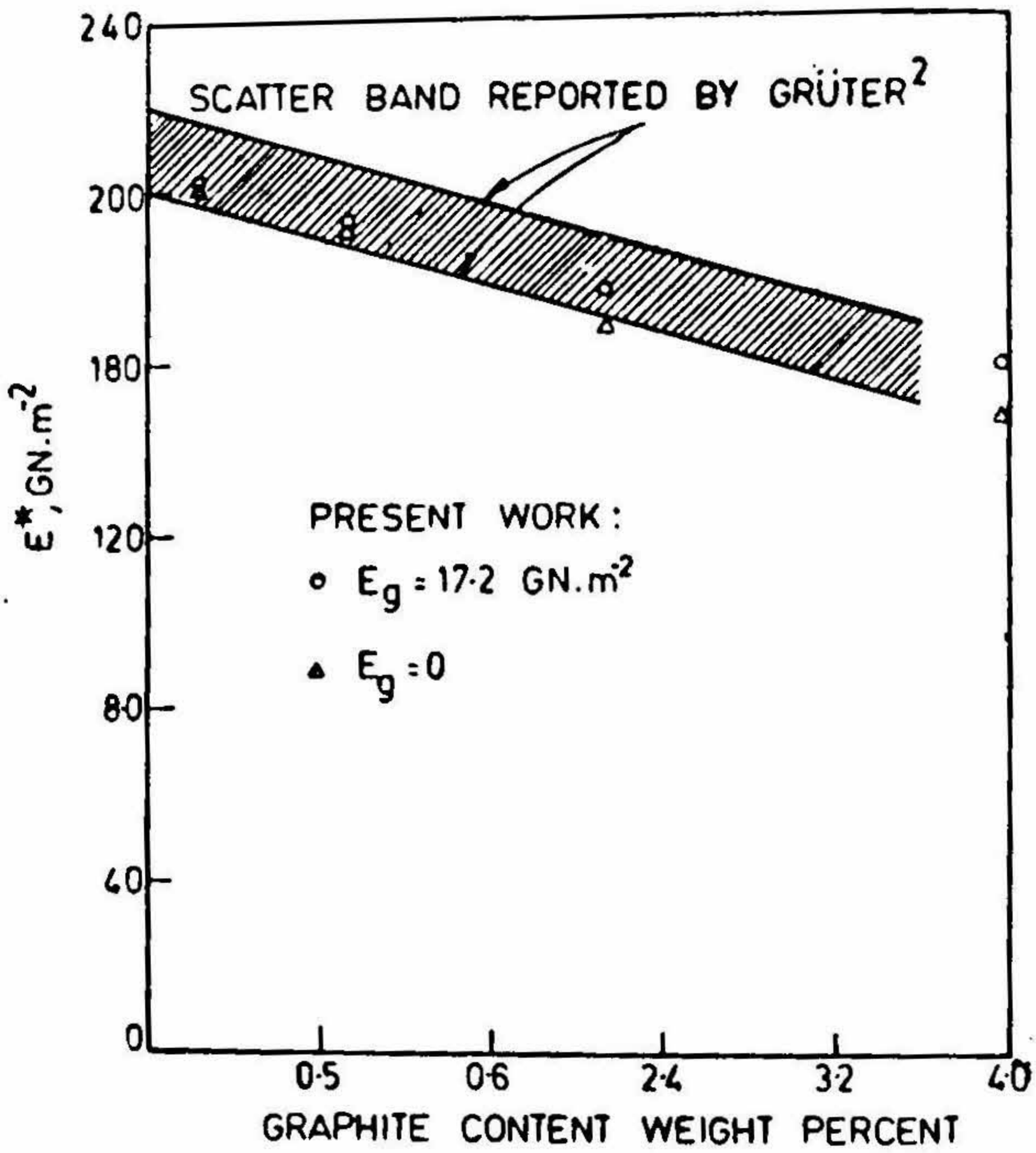

FIG. 6. Effect of graphite content upon overall elastic modulus.

modulus, the latter fact is well known in engineering composites[13]. Further, it is interesting to note that if the contact is partial, these advantages may be lost (Fig. 5) and with dcerease in the angle ofcontact, the results tend to be similar to those obtained when the inclusion is considered to be a void (Figs. 3 and 5). It is also noted that the E^* values obtained for b/a ratio in the range of 0·3 to 0·4 under rigid interface condition with full contact (Case 3, Fig. 3) are considerably higher than the reported values of the elastic modulus of spheroidal graphite cast iron. This suggests that a rigid interface condition is unlikely to prevail in spheroidal graphite cast iron and the observation that graphite in cast iron deforms under load[14,15] also lends support to this viewpoint.

Nomenclature

$2a$	..	Unit cell dimension
$2b$	..	Diameter of the inclusion

E_0, v_0 .. Elastic constants of the inclusion
E_m, v_m .. Elastic constants of the matrix
E^* v^* .. Overall elastic constants
V_0 .. Volume fraction of the inclusion
F_x, F_y .. Forces on the edges of unit cell
U_x, U_y .. Uniform displacements applied to unit cell

References

1. ANGUS, H. T. — *Cast iron : Physical and engineering properties*, Butterworths, London, 1976.
2. GRÜTER, L. — Prediction of fracture toughness of cast iron alloys, *Mater. Sci. Engng.*, 1978, 35, 157–164.
3. LOHE, D., VÖHRINGER, O. AND MACHERAUCH, E. — The influence of graphite shape on mechanical properties of ferritic cast iron ; In K. J. Miller and R. F. Smith (eds.), *Mechanical behaviour of materials*, Pergamon Press, Oxford, 1980, 3, 179–188.
4. RAO, A. K. — Elastic analysis of pin joints, *Computers Struct.*, 1978, 9, 125–144.
5. GHOSH, S. P. — Analysis of joints with elastic pins, *Ph.D. Thesis*, Indian Institute of Science, Bangalore, India, 1978.
6. MANGALGIRI, P. D. — Elastic analysis of pin joints with composite plates, *Ph.D. Thesis*, Indian Institute of Science, Bangalore, India, 1980.
7. DESAI, C. S. AND ABEL, J. F. — *Introduction to the finite element method*, Affiliated East-West Press, New Delhi, 1972.
8. PLENARD, E. — The elastic behaviour of cast iron ; In H. D. Merchant (ed.), *Recent research on cast iron*, Gordon and Breach, New York, 1968, pp. 707–792.
9. SHIBATA, M. AND ONO, K. — Stress concentration due to an oblate spheroidal inclusion, *Mater. Sci. Engng.*, 1978, 34, 131–137.
10. SEETHARAMU, S. AND SRINIVASAN, M. N. — Unpublished work, Indian Institute of Science, Bangalore, India.
11. GILBERT, G. N. J. AND EMERSON, P. J. — The elastic properties of cast irons determined statically and dynamically, Report 888, *B.C.I.R.A. J.*, 1967, 15, 436–457.
12. GILBERT, G. N. J. — Effect of carbon content on the mechanical properties of annealed ferritic nodular irons, Report 765, *B.C.I.R.A. J.*, 1964, 12, 791–807.
13. DIVECHA, A. P., FISHMAN, S. G. AND KARMARKAR, S. D. — Silicon carbide reinforced aluminium—A formable composite, *J. Metals*, 1981, 33(9), 12–17.
14. GILBERT, G. N. J. — The stress/strain properties of nodular cast irons in tension and compression, Report 730, *B.C.I.R.A. J.*, 1964, 12, 170–193.

15. RICKARDS, P. J. Ductile and brittle fracture in ferritic nodular graphite irons, *J. Iron Steel Inst.*, 1971, 209, 190–196.

Appendix

As the boundaries of the unit cell form axes of symmetry (Fig. 1) displacements normal to them are uniform and the shear stress is zero. For the applied uniform displacements U_x and U_y on edges BC and CD (Fig. 2), let the corresponding resisting forces be F_x and F_y. For a linearly elastic solid,

$$F_y = AU_x + BU_y$$

and $$F_x = CU_x + DU_y$$

(where A, B, C and D are constants. For a given set of displacements (U_{x1}, U_{y1}) and (U_{x2}, U_{y2}) the constants A, B, C and D can be evaluated in terms of forces. Choosing the set of displacements to be (1, 0) and (1, 1), it can be shown that

$$A = F_{y1},\ B = F_{y2} - F_{y1},\ C = F_{x1} \text{ and } D = F_{x2} - F_{x1}$$

where (F_{x1}, F_{y1}) and (F_{x2}, F_{y2}) correspond to displacements (1, 0) and (1, 1) respectively.

To find overall elastic constants E^* and ν^* a case of uniaxial tension in X-direction is considered. In such a case the net force transferred in Y-direction is zero and hence

$$F_y = AU_x + BU_y = O$$

The Poisson's ratio ν^* (which is defined as the ratio of Y-displacement to X-displacement for uniaxial tension in the X-direction) is therefore given by

$$\nu^* = U_y/U_x = -A/B = (F_{y1} - F_{y2})/F_{y1}.$$

The elastic modulus E^* is obtained by the ratio of stress to strain in the X-direction For a cell of unit thickness E^* is given by

$$E^* = \frac{F_x}{U_x} = C + D\frac{U_y}{U_x}$$

or $$E^* = F_{x1} + (F_{x2} - F_{x1})\ (F_{y1} - F_{y2})/F_{y1}$$